Reliability analysis of rotor blades of tidal stream turbines

Dimitri V. Val[a,*], Leon Chernin[b] and Daniil V. Yurchenko[c]

[a] *School of the Built Environment, Heriot-Watt University, Edinburgh EH14 4AS, United Kingdom*

[b] *School of Engineering, Physics and Mathematics, University of Dundee, Dundee DD1 4HN, United Kingdom*

[c] *School of Engineering & Physical Sciences, Heriot-Watt University, Edinburgh EH14 4AS, United Kingdom*

Abstract

Tidal stream turbines are used for converting kinetic energy of tidal currents into electricity. There are a number of uncertainties involved in the design of such devices and their components. To ensure safety of the turbines these uncertainties must be taken into account. The paper shows how this may be achieved for the design of rotor blades of horizontal-axis tidal stream turbines in the context of bending failure due to extreme loading. Initially, basic characteristics of such turbines in general and their blades in particular are briefly described. A probabilistic model of tidal current velocity fluctuations, which are the main source of load uncertainty, is then presented. This is followed by the description of reliability analysis of the blades, which takes into account uncertainties associated with tidal current speed, the blade resistance and the model used to calculate bending moments in the blades. Finally, the paper demonstrates how results of the reliability analysis can be applied to set values of the partial factors for the blade design.

Keywords: Tidal stream turbine, rotor blades, reliability, turbulence, partial safety factors

Highlights:

- A probabilistic model of the maximum of tidal current velocity fluctuations is proposed
- Reliability analysis of rotor blades of a tidal stream turbine is described
- Influence of pitch control system on the blade reliability is investigated
- Partial safety factors for the design of tidal turbine rotor blades are calibrated

[*] Corresponding author: Tel.: +44 1314514622; fax: +44 1314514617.
E-mail address: d.val@hw.ac.uk

1. Introduction

Tidal stream turbines are a relatively new technology for extracting kinetic energy from tidal currents, which is currently in transition from development stage to industrial implementation. A number of different concepts of such devices have been proposed so far and the most popular of them is a horizontal-axis turbine with propeller-type blades [1]. There are still no standards or other guidelines for the design of such devices in general and their rotor blades in particular. There are two types of limit states that may be of concern for the design of the rotor blades – ultimate and fatigue. However, it is expected that the design of rotor blades for tidal stream turbines will be controlled mainly by bending failure due to extreme loading as opposed to that for wind turbines where fatigue is the main cause of concern. This is supported, for example, by results presented by McCann et al. [2] who examined the influence of both extreme and fatigue loads on the design of blades for a generic tidal stream turbine. Of course, this does not mean that fatigue loading is completely unimportant for the design of such devices and there is no need to consider it.

The paper starts with a brief description of the main characteristics of tidal stream turbines with particular emphasis on horizontal-axis turbines with propeller-type blades. This is illustrated by an example of a generic horizontal-axis pitch controlled turbine, which is later employed to demonstrate the reliability assessment of the rotor blades. After that a probabilistic model of tidal current velocity fluctuations, which are the main source of load uncertainty, is presented. Since the rotor blades under consideration are pitch controlled it can be assumed that their overloading due to slow variations in the tidal current velocity is prevented by adjustment of the pitch angle. Thus, only variability of the tidal current velocity due to high frequency fluctuations caused by turbulence is modelled. The stochastic turbulence model is based on von Karman spectrum, which satisfies Kolmogorov's theory of turbulence and hence can be used to describe both sea [3] and wind turbulence [4].

Reliability analysis of the rotor blades in the context of bending failure due to extreme load during power production is then described. It should be noted that other ultimate limit states (e.g., local buckling) and design situations (e.g., fault conditions) may need to be considered in the rotor blade design; however, these are out of the scope of this paper. Uncertainties associated with tidal current speed, the blade resistance and the model used to calculate bending moments in the blades are taken into account. Only static behaviour of the blades is considered. Bending moments in the blades are calculated using the blade element-momentum theory. Finally, the paper shows how results of the reliability analysis can be

applied to determine values of the partial factors for the design of tidal turbine rotor blades with respect to bending failure.

2. Tidal stream turbines

2.1 Basic classification

Tidal stream turbines can be classified according to:

- rotor configuration – axial- or cross-flow, open or ducted;
- drive train configuration – indirect drive, when a rotor is connected to a generator via a gearbox, or direct drive, when a rotor is directly connected to a generator;
- type of supporting structure – fixed to the seabed, gravity based or floating.

Additional classifications based on other parameters are also possible. A majority of the turbines currently under development are horizontal axis (i.e. axial-flow) devices with an open rotor [1]; thus, similar to a typical wind turbine. An important parameter for this type of turbines is the way their blades are connected to the rotor hub. The blades can be fixed (fixed-pitch) or being made rotatable about their axes (variable pitch). In the latter case the blades' orientation towards the current flow direction can be changed and by this the power take-off can be controlled (pitch controlled turbine).

2.2 Performance characteristics

Performance of tidal stream turbines is usually characterised in terms of dimensionless coefficients such as the power coefficient, C_P

$$C_P = \frac{P}{\frac{1}{2}\rho U^3 \pi R^2} \tag{1}$$

and the coefficient of thrust, C_T

$$C_T = \frac{T}{\frac{1}{2}\rho U^2 \pi R^2} \tag{2}$$

where P is the power, T the thrust, R the radius of the rotor, U the speed of tidal current and ρ the density of seawater (≈1025 kg/m^3). The first coefficient represents the efficiency of a tidal turbine in converting kinetic tidal stream energy into mechanical energy. The second one represents the thrust acting on the turbine rotor and therefore is related to bending moments

in the rotor blades; for the same U the higher C_T the larger the bending moment at the root of the blade.

Both C_P and C_T are usually presented as a function of the tip speed ratio, λ, i.e. the ratio between the speed of the rotor blade tip and the current speed

$$\lambda = \frac{\Omega R}{U} = \frac{2\pi N_r R}{60U} \tag{3}$$

where Ω is the rotational speed of the rotor (rad/s) and N_r the number of the rotor rotations per minute (rpm).

In this paper a horizontal axis pitch-controlled turbine with a three-bladed rotor of 18-m diameter (i.e. $R = 9$ m) is considered. The turbine has a fixed rotational speed. The total water depth at the turbine location is 45 m and the height of the hub above the seabed is 21 m. The NREL S814 foil [5] is adopted for the blade section. Details of the blade geometry are given in Table 1, where r is the distance from the rotor axis and c the blade chord. Figure 1 shows C_P and C_T versus λ for the turbine. As can be seen, the turbine's performance is efficient when λ is in the range of 4 to 8 ($C_P > 0.4$). At the same time, lower values of C_T correspond to lower bending moments in the blades, hence, from this point of view the lower λ the better. It is necessary to note that this turbine (including the blade geometry) has been developed with the only purpose to illustrate a method for reliability analysis of rotor blades presented further in the paper. The design is not optimal and not intended for the use in real devices.

The results in Figure 1 are calculated using the NWTC Subroutine Library [6], which is based on the blade element momentum theory. The Prandtl tip-loss factor is used to account for tip and hub losses. The drag, C_d, and lift, C_l, coefficients for the blade elements are derived using the two-dimensional (2-D) vortex panel code XFoil [7]. Since XFoil is capable to calculate values of C_d and C_l only up to stall, their post stall values are estimated by the Viterna method [8]. To account for the effects of rotation on increasing lift and delaying stall the so-called 3-D correction method proposed by Snel et al. [9] is employed for each blade segment. It has been shown that loads on the rotor blades of tidal stream turbines predicted by this approach are in good agreement with experimental results [10], including cases when turbulence occurs [11]. The analysis also takes into account variation of the tidal current speed over the water column, which is described by the $1/7^{th}$ power law (e.g. [12]).

Another important issue is cavitation, which can cause significant wearing of turbine blades due to local continuous cyclic stressing of the blade surface. Cavitation occurs when

the local pressure, p_L, on the blade surface falls below vapour pressure of the sea water [13]. Consequently, cavitation inception can be predicted from the distribution of pressure around the blade foil by comparing the minimum negative pressure coefficient

$$C_p = \frac{p_L - (p_{AT} + \rho g h)}{0.5 \rho U^2} \tag{4}$$

with the cavitation number

$$Ca = \frac{p_{AT} + \rho g h - p_V}{0.5 \rho U^2} \tag{5}$$

where p_{AT} is the atmospheric pressure and p_V the vapour pressure of sea water; cavitation occurs when $-C_P > Ca$. It has been ensured that there will be no cavitation at the turbine blade tips by checking that $-C_p$ remains below Ca for the range of U between 1 and 5 m/s. The distribution of C_p around the foil has been calculated using XFoil [7] and taking into account the rotational velocity of the blade tip, the blade twist angle and changes in the pitch angle corresponding to various values of the current speed. For more information about cavitation and its prevention in tidal stream turbines see, e.g., [14], [15].

Figure 2 shows a power versus current speed curve for the turbine when the rated current speed is 2.6 m/s (rated current speed is a speed at which the turbine reaches its rated power); cut-in current speed is 1 m/s. The rotational speed of the rotor is 14 rpm that corresponds to $\lambda = 5.07$ at the rated current speed. The figure also shows the corresponding bending moments: flapwise (out-plane), in-plane and total, at the blade root.

The blade pitch angle is adjusted to achieve the maximum power at current speeds below the rated speed. At current speeds above the rated speed the pitch angle increases to reduce the angle of attack and limit the power to its rated value. The mechanical power on the shaft at the rated speed is 1000 kW; actual power is lower due to losses in a gearbox, generator, converter and transmission (the losses are typically around 15%, thus the actual rated power of the turbine is around 850 kW). As can been seen from Figure 2, the flapwise and total bending moments at the blade root reach their maximum at the rated current speed and then decrease rapidly as the pitch angle increases to keep the power constant. It can also be seen that at the peak the difference between these two moments is insignificant.

3. Probabilistic modelling of tidal current velocity fluctuations

3.1 Stochastic model of turbulence

The variation of current velocity over time t can be presented as the sum of the average velocity $\bar{U}(t)$ (usually averaged over 10-minute intervals) and fluctuations $u(t)$ caused by turbulence

$$U(t) = \overline{U}(t) + u(t) \tag{6}$$

It should be noted that the velocity fluctuations vary not only in time but also in space. However, for simplicity spatial variability of the fluctuations is not considered in this paper.

Since the turbine under consideration is pitch controlled the maximum bending moment at the blade root is reached when $\bar{U}(t)$ equals the rated current speed; at higher $\bar{U}(t)$ the bending moment decreases rapidly due to increasing pitch angle (see Figure 2). Thus, slow variations in $\bar{U}(t)$ cannot cause overloading of the blades and, therefore, are not of concern. Moreover, if the pitch control system fails then there is a spring that forces the blades out of the direction of the tidal stream flow. This in combination with subsequent shut down of the turbine should prevent, in principle, overloading of the blades in case of failure of the control system. Further consideration of the latter design situation may still be needed but this is outside the scope of the present paper. At the same time, the pitch control system cannot react fast enough to high frequency fluctuations $u(t)$ that may lead to much higher bending moments at the blade root than the ones shown in Figure 2. Thus, to estimate the reliability of the rotor blades in the context of bending failure a probabilistic model of the velocity fluctuations is needed, or more exactly, the model of the maximum fluctuation which will coincide with the rated current speed and occur during the service life of the turbine.

Turbulence is usually characterised by its intensity, I_u, which is defined as the ratio of the standard deviation of the velocity fluctuations, σ_u, to the average velocity, i.e.

$$I_u = \frac{\sigma_u}{\overline{U}} \tag{7}$$

According to available data, I_u depends on the average current velocity and during slack periods may reach 50%; however, it significantly decreases with an increase in $\bar{U}$. For current velocities faster than 1.5 m/s I_u is about 10% [2], [15], [16]. The turbulence intensity also varies with the height above the seabed (e.g. [15]) but this is not considered in this paper.

Another characteristic of turbulence required in various turbulence models is the integral length scale, L. There are limited data about this characteristic. It has been suggested

that for an open channel L can be set approximately equal to 0.8 of the channel depth [17]. The total depth at the turbine location is 45 m; hence, it assumed in the following calculations that L=0.8×45=36 m. It is worth to note that according to available results bending moments at the blade root are not very sensitive to values of L [18].

Stochastic properties of turbulence can be described by its power spectrum (or spectral density), $S_u(f)$, which is obtained by the Fourier transform of the autocorrelation of $u(t)$, where f represents the frequency of fluctuations. According to Kolmogorov's theory, turbulence power spectra should become proportional to $f^{-5/3}$ as f increases (e.g. [3]). There are a number of spectra which satisfy this condition, including von Karman and Kaimal spectra which are widely used to describe wind turbulence [4]. Results reported in [18] show that the choice of any of these two spectra has insignificant effect on the evaluation of loads in the tidal turbine blades. In this paper the tidal flow turbulence is described by the von Karman spectrum, which in non-dimensional form can be expressed by as

$$\frac{fS_u(f)}{\sigma_u^2} = \frac{\frac{4fL}{\overline{U}}}{\left[1+70.78\left(\frac{fL}{\overline{U}}\right)^2\right]^{5/6}} \tag{8}$$

It is also assumed that $u(t)$ is a stationary Gaussian process with zero mean and standard deviation σ_u.

A factor, which needs to be considered in developing a stochastic turbulence model for reliability analysis of a pitch controlled tidal stream turbine, is that a pitch control system may react to low frequency velocity fluctuations by adjusting the pitch angle and reducing the root bending moment. This depends on the pitch response cut-off frequency, f_{pc}, which is normally lower than the rotational frequency of the rotor. To account for this the standard deviation of the velocity fluctuations, σ_u, should be replaced by its reduced value, $\sigma_{u,c}$, which is estimated as

$$\sigma_{u,c} = \sqrt{\int_{f_{pc}}^{\infty} S_u(f)df} \tag{9}$$

3.2 Maximum of fluctuations over a time interval of finite duration

The largest bending moments act at the blade root when $\bar{U}(t)$ is close to the rated current speed, U_r (see Figure 2). Time intervals over which $\bar{U}(t)\approx U_r$ are of relatively short

duration and occur regularly during the service life of a tidal stream turbine (up to four times per day in a semi-diurnal tide). The maximum bending moment at the blade root will be during these intervals when $u(t)$ reaches its maximum value in the direction of $\bar{U}(t)$. The distribution of the maximum value of $u(t)$ can be derived in the following way. First, the distribution of the maximum of $u(t)$, u_{max}, within a time interval, t_{int}, when $\bar{U}(t) \approx U_r$ needs to be established, which will be considered in this section. The distribution of the maximum of these interval maxima for all such intervals during the turbine (or blade) life then needs to be formulated that will be addressed in in the next section.

A Gaussian stationary process with a von Karman power spectrum is non-differentiable and there is no closed form formula for the distribution of its maximum over a finite time interval (e.g., [19]). However, it can be shown that since its covariance function satisfies certain conditions its maximum is well defined and finite for any duration of the time interval. Moreover, as the duration of the time interval increases the distribution of the maximum converges asymptotically to the Extreme Value Type 1 (Gumbel) distribution (see Appendix A).

In the paper, parameters and the type of the distribution of $u_{\max}(t_{int})$ are estimated numerically using Monte Carlo simulation. Samples of $u(t)$ have been generated using the inverse Fourier transform (e.g. [20]) for eleven time intervals between 60 s and 900 s. For each time interval 10,000 samples have been generated and the mean, $\mu_{u,max}$, and standard deviation, $\sigma_{u,max}$, of the maximum of $u(t)$ over the interval have been estimated. Results of the analyses normalised by the standard deviation σ_u are shown in Figure 3. As can be seen, the relationships between these normalised statistical parameters of u_{max} and t_{int} can be well described by logarithmic functions

$$\frac{\mu_{u,max}(t_{\text{int}})}{\sigma_u} = 0.443\ln(t_{\text{int}}) + 0.239 \tag{10}$$

$$\frac{\sigma_{u,max}(t_{\text{int}})}{\sigma_u} = -0.090\ln(t_{\text{int}}) + 1.030 \tag{11}$$

where t_{int} is in seconds.

To assess what distribution type represents better the distribution of $u_{\max}(t_{int})$ probability plots have been built using the generated data. Results for two distribution types: normal and Gumbel, are shown in Figure 4. It can been observed that for relatively short time intervals (up to t_{int}= 600 s) the distribution of $u_{max}(t_{int})$ is very well approximated by a normal distribution, while for a longer interval (t_{int}= 900 s) the Gumbel distribution fits slightly better

to the generated data. The results demonstrate that in accordance to the theory (see Appendix A) the distribution of $u_{max}(t_{int})$ slowly converges to the Gumbel distribution as t_{int} increases. However, for relatively short time intervals a normal distribution provides a sufficiently good approximation and can be used to represent the distribution of $u_{max}(t_{int})$ along with the values of the mean and standard deviation given in Figure 3.

3.3 Maximum of fluctuations over the service life of a tidal stream turbine

Since the maximum bending moment occurs when $u(t)$ reaches its maximum in the same direction as $\bar{U}(t)$, while the latter should be close to U_r, it is necessary to know on how many occasions during the turbine service life $\bar{U}(t) \approx U_r$ and what the duration of such periods is. In probabilistic terms this means that the distribution of the maximum of $u_{max}(t_{int})$ over m time intervals, each of duration t_{int}, is needed, where m is the number of time intervals during the service life of a turbine (or any other time period under consideration) at which $\bar{U}(t) \approx U_r$. This distribution of the maximum, $F_{U,m}$, can be expressed as

$$F_{U,m}(u) = \left[F_{U,max}(u)\right]^m \tag{12}$$

where $F_{U,max}$ is the distribution of $u_{max}(t_{int})$ for a given duration of the time interval, t_{int}.

If t_{int} is relatively short ($\leq$ 600 s), as has been shown previously $u_{\max}(t_{int})$ can be modelled by a normal distribution and since m is expected to be sufficiently large, the distribution of the maximum of $u_{max}(t_{int})$ over m time intervals can be approximated by the Gumbel distribution (e.g., [21])

$$F_{U,m}(u) = \exp\left\{-\exp\left[-\alpha_m\left(\frac{u-\mu_{u,max}}{\sigma_{u,max}} - v_m\right)\right]\right\} \tag{13}$$

with the following parameters

$$\alpha_m = \sqrt{2\ln m}; \quad v_m = \alpha_m - \frac{\ln(\ln m) + \ln(4\pi)}{2\alpha_m} \tag{14}$$

If t_{int} is longer than 600 s, $u_{\max}(t_{int})$ can be modelled by the Gumbel distribution and the distribution of the maximum of $u_{max}(t_{int})$ over m time intervals is then modelled by the Gumbel distribution as well but expressed in a slightly different form compared to Eqs. (13), (14)

$$F_{U,m}(u) = \exp\left\{-\exp\left[-\alpha_m'(u - v_m')\right]\right\} \tag{15}$$

where

$$\alpha_m' = \frac{\pi}{\sigma_{u,max}\sqrt{6}}; \quad v_m' = \mu_{u,max} - \frac{\gamma - \ln m}{\alpha_m'} \tag{16}$$

and γ =0.577216.

4. Reliability analysis of rotor blades

4.1 Reliability assessment: bending failure due to extreme load

To estimate the reliability (or its complement, the probability of failure) of a structural component by direct probabilistic analysis, a model describing failure of the component is needed. Uncertain parameters of the model, including uncertainty of the model itself, are treated as basic random variables. The model is then used to formulate the limit state function, G, in such a way that $G \leq 0$ corresponds to failure of the component. The limit state function is a function of the basic random variables, $\mathbf{X}$, and the probability of failure, P_f, of the component is estimated as

$$P_f = \Pr[G(\mathbf{x}) \leq 0] \tag{17}$$

where Pr[…] denotes the probability and $\mathbf{x}$ – particular values of the random variables $\mathbf{X}$.

For bending failure of a rotor blade at its root (see Figure 5) the limit state function can be expressed as

$$G(\mathbf{x}) = f_c - \frac{C_m M_f}{Z_f} \tag{18}$$

where f_c is the strength of the spar material, M_f the flapwise bending moment at the blade root, Z_f the section modulus of the spar about the corresponding axis, and C_m the parameter representing uncertainty associated with the evaluation of M_f using the blade element momentum theory. In principle, it would be more correct to calculate stresses in the spar caused by the total bending moment but, as has been seen from the results in Figure 2, the difference between the maximum values of M_f and M_t is negligible. Of courses, stresses depend not only on the bending moments but also on the corresponding section moduli; if the section modulus, Z_o, corresponding to the in-plane bending moment, is much smaller than Z_f then stresses caused by M_o may also be important. However, this cannot be the case when the blade spar has a box section (as in Figure 5); due to cross-sectional dimensions of the blade Z_o is usually similar to, or even larger than Z_f. The spar is made of composite laminate (glass or carbon fibre). Its strength in the direction of fibres can be represented by a lognormal random variable with a coefficient of variation (COV) of 0.10 [22].

There are multiple sources of uncertainty/error associated with the evaluation of forces acting on the turbine blades by the blade element momentum theory. The theory is based on the assumption that there is no radial interaction between the flows passing through continuous annuli of the disk defined by rotating rotor blades. Forces on a blade element are calculated using the lift and drag coefficients found from 2-D wind tunnel test data or, like in this research, 2-D analysis. A number of engineering corrections (see above) have been introduces to overcome the limitations of the theory and improve predictions; however, the agreement between the predictions and test results (or field measurements) is obviously far from perfect. In this study all these uncertainties are taken into account by a single random variable C_m. It has been estimated that for wind turbines the coefficient of variation of values of load effects (e.g., bending moments in rotor blades) due to the use of the blade element momentum theory for their calculation should be around 0.10-0.15 [23]. Thus, it is assumed herein that C_m is a normal random variable with a mean of unity and COV = 0.15. In principle, turbulence modelling, which ideally should be based on data collected during the site assessment, is another source of model uncertainty. However, no information is currently available to quantify this uncertainty.

As has been previously explained, the maximum of the velocity fluctuations over the service life of a tidal stream turbine can be modelled by the Gumbel distribution. However, the distribution parameters depend on the duration of a time interval during which $\bar{U}(t) \approx U_r$. For the turbine considered in the paper the rated current speed is U_r=2.6 m/s. It is assumed for illustrative purposes that the spring and neap tidal velocities are 3.1 m/s and 1.6 m/s, respectively. If to neglect effects of waves and wind on $\bar{U}(t)$ it is estimated that $\bar{U}(t)$ will be within the range $U_r \pm 0.05$ m/s around 1000 times per year, on average 600 s per time (i.e., m=1000 and t_{int}=600 s). For t_{int}=600 s the Gumbel distribution given by Eqs. (13), (14) should be used with $\mu_{u,max}$=0.79 m/s and $\sigma_{u,max}$=0.12 m/s (the latter values are taken from Figure 3).

To carry out reliability analysis a relationship between M_f and the tidal current speed needs to be established. The relationship obviously depends on the pitch angle of the blade. However, as should be clear from the previous discussion maximum values of the bending moment occur when the turbine is operating at a rated current speed; thus, the relationship between M_f and U is only needed for the pitch angle corresponding to this situation. For a wide range of the current speed around its rated value (i.e., 2.6 m/s) the relationship between M_f and U can be described sufficiently accurate by a linear function (see Figure 6):

$$M_f = 523U - 459 \text{ (kNm)} \tag{19}$$

where U is in m/s. Thus, the limit state function, Eq. (18), can be re-written in the following form

$$G(f_c, C_m, u_n) = f_c - \frac{C_m[A(U_r + u_m) - B]}{Z_f} \tag{20}$$

where $A = 523$ and $B = 459$; in this formula U_r and u_m are in m/s, Z_f in m^3 and f_c in kN/m^2. Since the distribution of u_m has been derived for a one-year period the reference time for Eq. (20) is one year as well.

The spar has a box section with external dimensions 665×425 mm and the wall thickness of 40 mm. The section modulus of the spar Z_f=7.3×10^{-3} m^3. It is assumed in this example that mean value of the composite strength is 350 MPa. The annual and cumulative probabilities of failure of the blade due to bending have been calculated for 20 years of the turbine service life using Monte Carlo simulation. Results of the analysis are shown in Figure 7. As can be seen, the highest annual probability of failure of the blade is during the first year of service. After that the annual probability of failure constantly decreases with time as the blade bending resistance is proven by loads experienced by the blade in the previous years, i.e., the annual probability is conditional on survival up to the time considered. It should be noted that these results have been obtained under the assumption that the bending resistance of the blade does not deteriorate with time.

As has been noted previously, the pitch control system reacts to low frequency current velocity fluctuations that may reduce significantly the fluctuations' variability and, subsequently, the variability of load on the blades. This depends on the pitch response cut-off frequency, f_{pc} – see Eq. (9). The pitch control system responds to velocity fluctuations with the frequency below f_{pc} by adjusting the pitch angle of the blades that prevents an increase in the root bending moment that could be caused by these fluctuations. For example, if f_{pc}=0.1 Hz (slightly below half of the rotational frequency of the rotor) then the standard deviation of the velocity fluctuations that should be considered in the analysis reduces from 0.26 m/s to 0.097 m/s. To examine this influence of the pitch control system on the reliability of the rotor blades the annual probability of bending failure of the blades has been calculated versus a range of values of f_{pc} for the turbine under consideration. Results are shown in Figure 8. As can be seen, a fast-reacting pitch control system (i.e., responding to fluctuations with the period of 120 s or less) enables to significantly reduce overload of the blades and their probability of failure (by one order of magnitude or more).

4.2 Calibration of partial safety factors

In ultimate limit state design the following criterion must be satisfied

$$S_d \leq R_d \tag{21}$$

where R_d is the design resistance and S_d the design load effect. In the context of bending failure of a tidal turbine blade

$$R_d = \frac{f_{c,k}}{\gamma_m}; \quad S_d = \gamma_f \frac{M_f}{Z_f} \tag{22}$$

where $f_{c,k}$ is the characteristic strength of the spar material, γ_m the partial factor for material and γ_f the partial factor for load. Taking into account Eq. (22), the criterion, Eq. (21), can be written in the following form

$$SF = \gamma_f \gamma_m \geq \frac{f_{c,k} Z_f}{M_f} \tag{23}$$

where SF is the product of the partial factors, which can be referred to as the safety factor. Since it has been assumed that f_c has a lognormal distribution its characteristic value defined as a low 5% quantile of the distribution is given by

$$f_{c,k} = f_{c,m} \exp\left(-1.645 COV_f\right) \tag{24}$$

where $f_{c,m}$ is the mean value of the tensile strength and COV_f its coefficient of variation (=0.10).

The reliability of a structural component is often expressed in terms of the reliability index β, which is related to the probability of failure by the following formula $\beta = -\Phi^{-1}(P_f)$, where Φ is the cumulative function of the standard normal distribution. Using Monte Carlo simulation, values of the reliability index associated with bending failure of the tidal turbine blade have been calculated as a function of the safety index and the results are presented in Figure 9.

In order to select a required value of SF the target reliability of a turbine blade in bending needs to be specified. An annual probability of failure of 1×10^{-4} (corresponds to $\beta = 3.7$) is a typical target value for structures with medium consequences of failure (e.g. [24]). Two cases are considered. In the first one, to demonstrate the effect of current velocity fluctuations due to turbulence on the reliability of tidal turbine blades the nominal load effect (i.e., M_f/Z_f) corresponds to average load, i.e., it is based on average current velocity and does not account for any influence of the velocity fluctuations. If the target reliability index $\beta_T = 3.7$ then SF should be at least 2.6 (see Figure 9) that in terms of the partial factors can be

achieved by setting, e.g., $\gamma_m = 1.3$ and $\gamma_f = 2.0$. It is logical to select a lower value for the partial factor for material since uncertainty associated with the blade resistance is much lower than that of the load effect. The resulting partial safety factors are high, especially for load ($\gamma_f = 2.0$). In the second case, the nominal load effect corresponds to characteristic load obtained for the current velocity with the return period of 50 years (the magnitude of the velocity fluctuations, for which the annual probability of being exceeded is 0.02, equals 1.29 m/s). SF should then be greater than 1.48 (see Figure 9) and the partial safety factors can be selected as $\gamma_m = 1.1$ and $\gamma_f = 1.35$, i.e., similar to the values used in the design of wind turbine blades.

The partial factors may also be reduced by taking into account a decrease in the standard deviation of the current velocity fluctuations due to adjustments of the blade pitch angle by the pitch control system. However, in this case the partial factors (or the one for load) will depend on the pitch response cut-off frequency that is undesirable.

5. Conclusions

Various concepts of tidal stream turbines have been briefly described. The main parameters used to characterise their performance have been introduced and their evaluation has been illustrated for a horizontal axis pitch-controlled turbine. A probabilistic model describing the maximum of current velocity fluctuations due to turbulence has been developed. An approach for the reliability assessment of rotor blades of this type of turbine in the context of bending failure has then been presented. It is important to stress that the probabilistic model which has been employed to represent uncertainty associated with the evaluation of bending moments is only suitable for pitch-controlled devices and should not be used for stall-controlled turbines. The approach has been used to calibrate the partial factors for the ultimate limit state design of tidal turbine blades in bending.

Appendix A. Maximum of a stationary Gaussian process with von Karman spectrum

The maximum of a non-differentiable stationary normal process (with zero mean and unit variance) is well defined and finite for any time interval t_{int} if the autocorrelation function of the process, $\rho(t)$, satisfies the following condition [21]

$$\rho(t) = 1 - C|t|^{\alpha} + o\left(|t|^{\alpha}\right) \text{ as } t \to 0 \tag{A.1}$$

where α is a constant, $0 < \alpha \leq 2$, and C a positive constant.

The autocorrelation function is related with the power spectrum through Fourier transform

$$\rho(t) = \int_0^\infty S_u(f)\cos(2\pi f t)df \tag{A.2}$$

For the von Karman spectrum given by Eq. (8) the autocorrelation function is

$$\rho(t) = \frac{2\sigma_u^2}{\Gamma(1/3)}\left(\frac{t/2}{J}\right)^{1/3} \mathrm{K}_{1/3}\left(\frac{t}{J}\right) \tag{A.3}$$

where $\Gamma(.)$ is the Gamma function, $\mathrm{K}_{1/3}(.)$ the modified Bessel function of the second kind and order of 1/3, and

$$J = \frac{\Gamma(1/3)}{\Gamma(5/6)\sqrt{\pi}}\frac{L}{\overline{U}} \cong 1.34\frac{L}{\overline{U}} \tag{A.4}$$

$\mathrm{K}_{1/3}(t/J)$ in series representation can be expressed as (e.g. [25])

$$\mathrm{K}_{1/3}\left(\frac{t}{J}\right) = \frac{\pi}{2\sin(\pi/3)}\sum_{k=0}^{\infty}\frac{\left(\frac{t}{2J}\right)^{2k}}{k!}\left[\frac{\left(\frac{t}{2J}\right)^{-1/3}}{\Gamma\left(k+\frac{2}{3}\right)} - \frac{\left(\frac{t}{2J}\right)^{1/3}}{\Gamma\left(k+\frac{4}{3}\right)}\right] \tag{A.5}$$

Without loss of generality, assume that σ_u=1 and show that the autocorrelation function given by Eq. (A.3) satisfies the condition in Eq. (A.1). When $t \to 0$, all terms of the series in Eq. (A.5) higher than the first one (i.e., k = 0) can be neglected. Substituting Eq. (A.5) with only the first term in the series into Eq. (A.3) leads to

$$\begin{aligned}\rho(t) &= \frac{2}{\Gamma(1/3)}\left(\frac{t}{2J}\right)^{1/3}\frac{\pi}{2\sin(\pi/3)}\left[\frac{\left(\frac{t}{2J}\right)^{-1/3}}{\Gamma(2/3)} - \frac{\left(\frac{t}{2J}\right)^{1/3}}{\Gamma(4/3)}\right] \\ &= \frac{\pi}{\Gamma(1/3)\Gamma(2/3)\sin(\pi/3)} - \frac{\pi}{\Gamma(1/3)\Gamma(4/3)\sin(\pi/3)}\left(\frac{1}{2J}\right)^{2/3} t^{2/3} = 1 - Ct^{\alpha}\end{aligned} \tag{A.6}$$

where α=2/3 and

$$C = \frac{\pi}{\Gamma(1/3)\Gamma(4/3)\sin(\pi/3)}\left(\frac{1}{2J}\right)^{2/3} \tag{A.7}$$

Thus, the condition, Eq. (A.1), is satisfied.

The maximum has an Extreme Type 1 (Gumbel) limiting distribution (at $t \to \infty$) if [21]

$$\rho(t)\ln(t) \to 0 \text{ as } t \to \infty \tag{A.8}$$

It will be shown that this condition is satisfied as well. The modified Bessel function $K_{1/3}(.)$ can be asymptotically expanded for large arguments as [25]

$$\mathrm{K}_{1/3}\left(\frac{t}{J}\right) \approx \frac{B_0}{\sqrt{t}} e^{-t}\left(1+\frac{B_1}{t}+\frac{B_2}{t^2}+\frac{B_3}{t^3}+\right) \tag{A.8}$$

where B_0, B_1, B_2, B_3 are constants. Then

$$\begin{aligned}\rho(t)\ln(t) &\approx \frac{2}{\Gamma(1/3)}\left(\frac{t}{2J}\right)^{1/3}\frac{B_0}{\sqrt{t}} e^{-t}\left(1+\frac{B_1}{t}+\frac{B_2}{t^2}+\frac{B_3}{t^3}+\right)\ln t \\ &= C_1 t^{-1/6} e^{-t}\left(1+\frac{B_1}{t}+\frac{B_2}{t^2}+\frac{B_3}{t^3}+\right)\ln t\end{aligned} \tag{A.9}$$

Since

$$\lim_{t\to\infty} t^{-1/6} e^{-t} \ln t = 0 \tag{A.10}$$

obviously Eq. (A.9) $\to 0$ when $t \to \infty$.

References

[1] King J, Tryfonas T. Tidal stream power technology – state of the art. In: Proceedings of Oceans'09 IEEE. Bremen, Germany; 2009.

[2] McCann G, Thomson M, Hitchcock S. Implications of site-specific conditions on the prediction of loading and power of a tidal stream device. In: Proceedings of ICOE 2008. Brest, France; 2008.

[3] Thorpe SA. An Introduction to Ocean Turbulence. Cambridge University Press; 2007.

[4] British Standard. Wind turbine generator systems – Part 1: Safety requirements. BS EN 61400-1; 2004.

[5] Somers DM. The S814 and S815 Airfoils. Airfoils, Inc., State College, PA; 1992.

[6] Buhl ML. NWTC Design Codes (NWTC Subroutine Library); 2004. [Online]: http://wind.nrel.gov/designcodes/miscellaneous/nwtc_subs/

[7] Drela M. XFoil: An analysis and design system for low Reynolds number airfoils. In: Proceedings of the Conference on Low Reynolds Number Aerodynamics. University of Notre Dame, Indiana; 1989.

[8] Viterna LA, Corrigan RD. Fixed pitch rotor performance of large horizontal axis wind turbines. In: Proceedings of the DOE/NASA Workshop on Large Horizontal Axis Wind Turbines. Cleveland, OH; 1981.

[9] Snel H, Houwidnk R, Bosschers J. Sectional prediction of lift coefficients in rotating wind turbine blades in stall. Report ECN-C-93-052, Energy research Centre of the Netherlands, Petten; 1994.

[10] Batten WMJ, Bahaj AS, Molland AF, Chaplin JR. The prediction of the hydrodynamic performance of marine current turbines. Renewable Energy, 2008; 33(5), 1085-96.

[11] Corsar M. Turbulent loads upon tidal turbines: Comparison between experimental and modeling predictions. In: Proceedings of AWTEC 2012, paper B6-3. Jeju Island, Korea; 2012.

[12] HSE. Environmental considerations. Offshore Technology Report 2001/010, Health & Safety Executive, Norwich; 2002.

[13] Molland AF, Bahaj AS, Chaplin JR, Batten WMJ. Measurements and predictions of forces, pressures and cavitation on 2-D sections suitable for marine current turbines. Proc. of the Institution of Mechanical Engineers, Part M: Journal of Engineering for the Maritime Environment 2004; 218, 127-38.

[14] Batten WMJ, Bahaj AS, Molland AF, Chaplin JR. Hydrodynamics of marine current turbines. Renewable Energy, 2006; 31(2), 249-56.

[15] Thompson J, Polagye B, Richmond M, and Durgesh V. Quantifying turbulence for tidal power applications. In: Proceedings of Oceans'10 MTS/IEEE, paper 100514-042. Seattle, USA; 2010.

[16] Osalusi E. Analysis of wave and current data in a tidal energy test site. Ph.D. thesis, Heriot-Watt University, Edinburgh, UK; 2010.

[17] Nezu I, Nakagawa H. Turbulence in Open-Channel Flows. Balkema; 1993.

[18] Milne IA, Sharma RN, Flay RGJ, and Bickerton S. The role of onset turbulence on tidal turbine blade loads. In: Proceedings of the 17th Australasian Fluid Mechanics Conference. Auckland, NZ; 2010.

[19] Azaïs JM, Wschebor M. The distribution of the maximum of a Gaussian process: Rice method revisited. In: In and Out of Equilibrium. Birkhäuser, Boston, MA; 2002. p. 321-48.

[20] Grigoriu M. A spectral representation based model for Monte Carlo simulation. Probabilistic Engineering Mechanics 2000; 15, 365-70.

[21] Leadbetter MR, Lindgren G, Rootzén H. Extremes and Related Properties of Random Sequences and Processes. Springer-Verlag; 1983.

[22] Ronold KO, Larsen GC. Reliability-based design of wind-turbine rotor blades against failure in ultimate loading. Engineering Structures 2000; 22, 565-74.

[23] Veldkamp HE. Chances in Wind Energy: A Probabilistic Approach to Wind Turbine Fatigue Design. PhD thesis, Delft University of Technology, Delft, Netherlands; 2006.

[24] DNV. Guideline for offshore structural reliability analysis – General. DNV Report 95-2018. Det Norske Veritas; 1995.

[25] Abramowitz A, Stegun IA, eds. Handbook of Mathematical Functions. National Bureau of Standards Applied Math. Series 55; 1964.

List of figures

Table 1. Details of the blade geometry.

r/*R*	*c*/*R*	Twist (^{o})
0.225	0.20	21.5
0.275	0.18	18.0
0.325	0.14	13.0
0.375	0.13	11.0
0.425	0.12	9.0
0.475	0.12	9.0
0.525	0.12	8.0
0.575	0.12	8.0
0.625	0.12	7.0
0.675	0.12	7.0
0.725	0.11	6.0
0.775	0.11	6.0
0.825	0.11	6.0
0.875	0.11	6.0
0.925	0.08	5.0
0.975	0.05	4.0

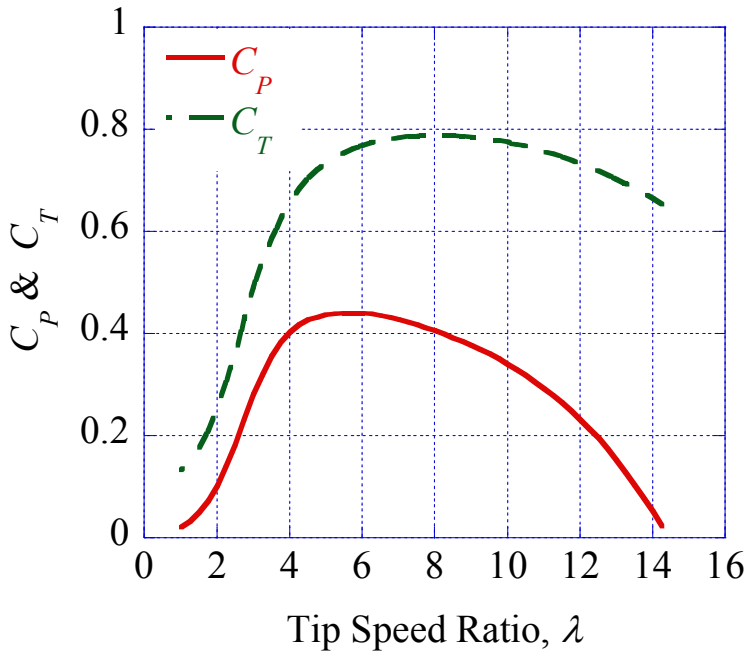

Figure 1. Power and thrust coefficients for the turbine.

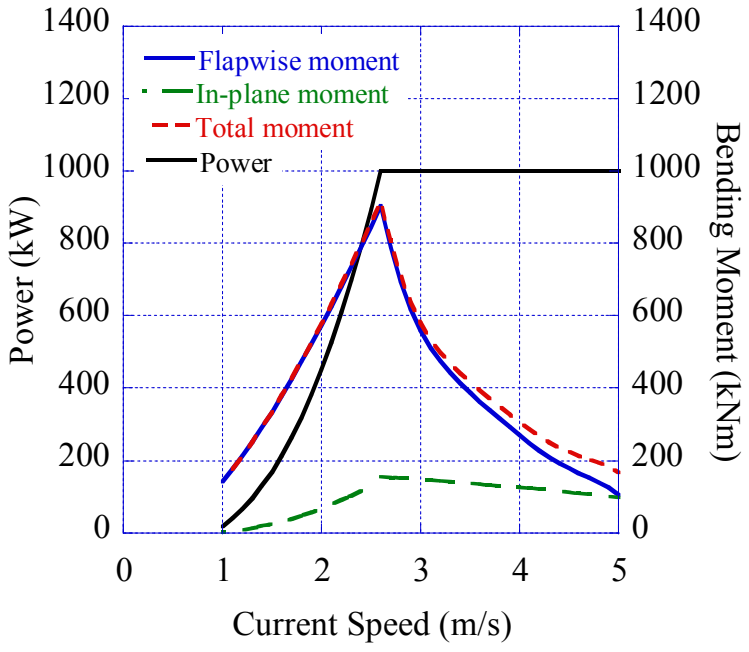

Figure 2. Power and bending moments at the blade root vs. tidal current speed.

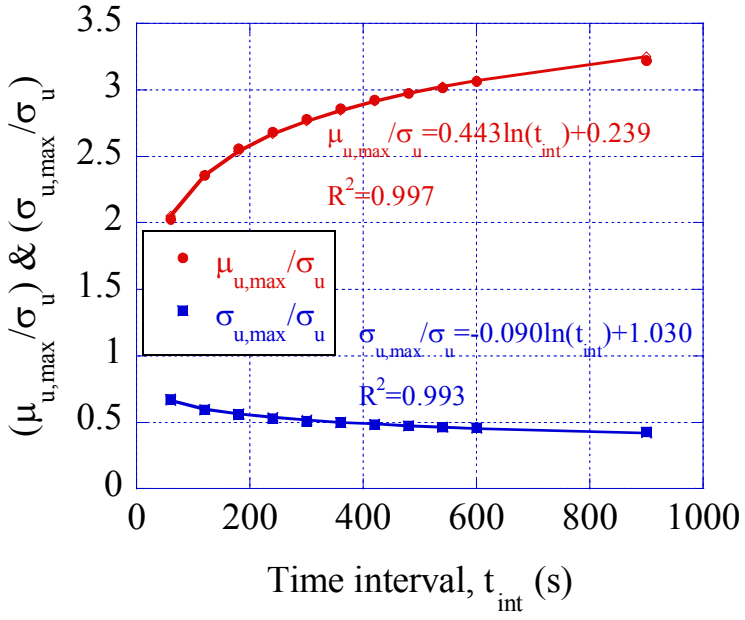

Figure 3. Relationships between mean and standard deviation of the maximum of velocity fluctuations and duration of the corresponding time interval.

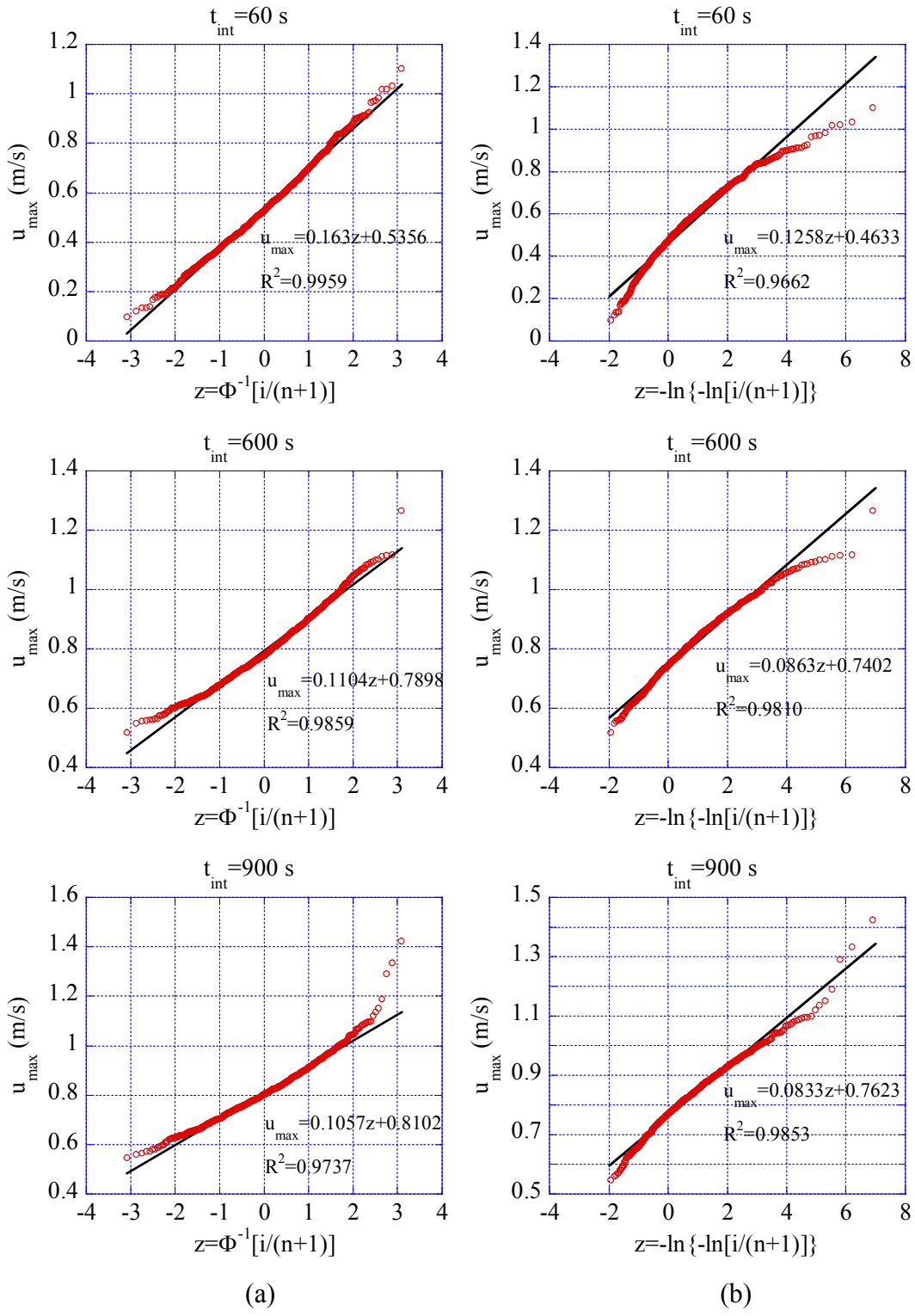

Figure 4. Probability plots based on generated values of $u_{max}(t_{int})$: (a) normal distribution; (b) Gumbel distribution.

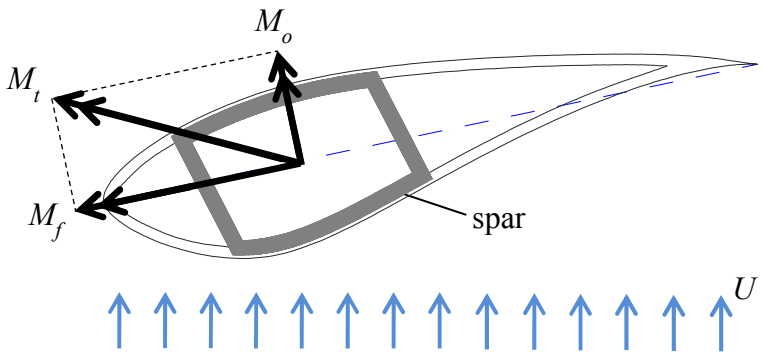

Figure 5. Blade cross-section at the root with acting bending moments: M_f – flapwise moment, M_o – in-plane moment and M_t – total moment.

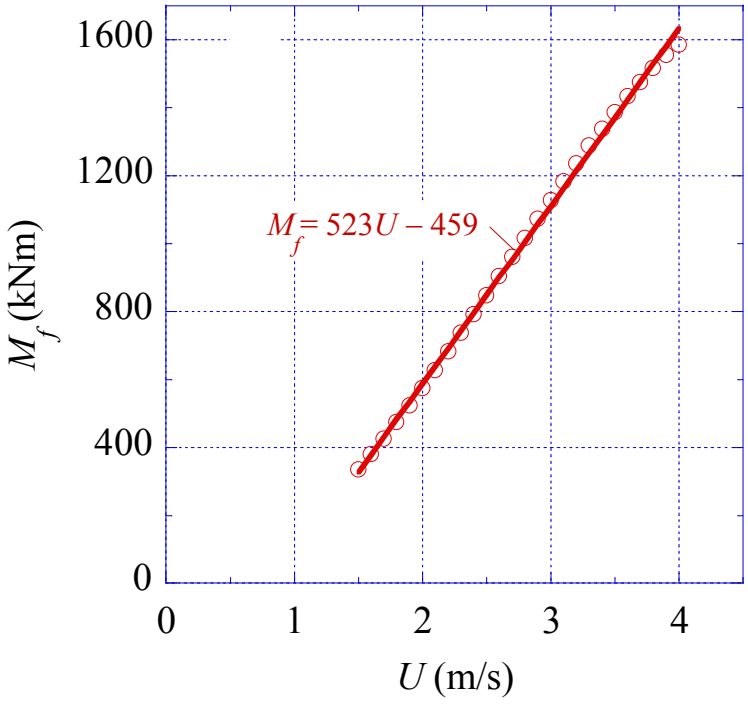

Figure 6. Relationship between flapwise bending moment and tidal current speed.

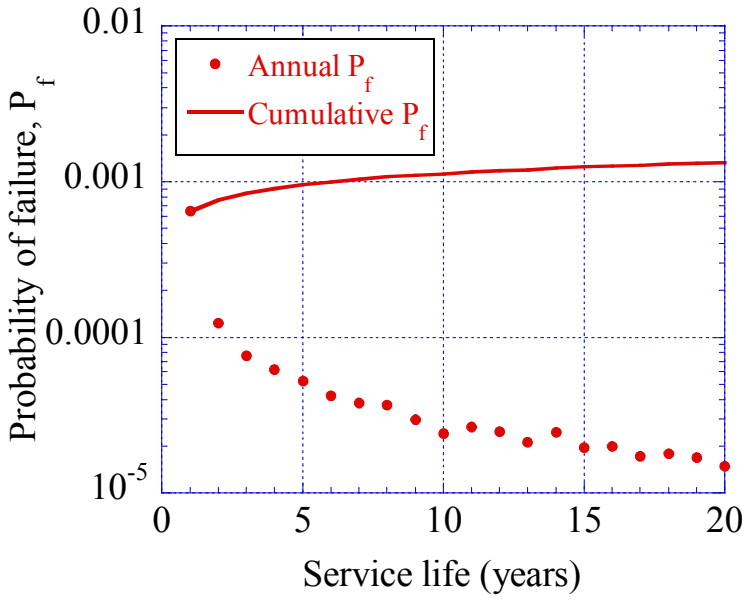

Figure 7. Annual and cumulative probabilities of bending failure of the blade due to extreme load.

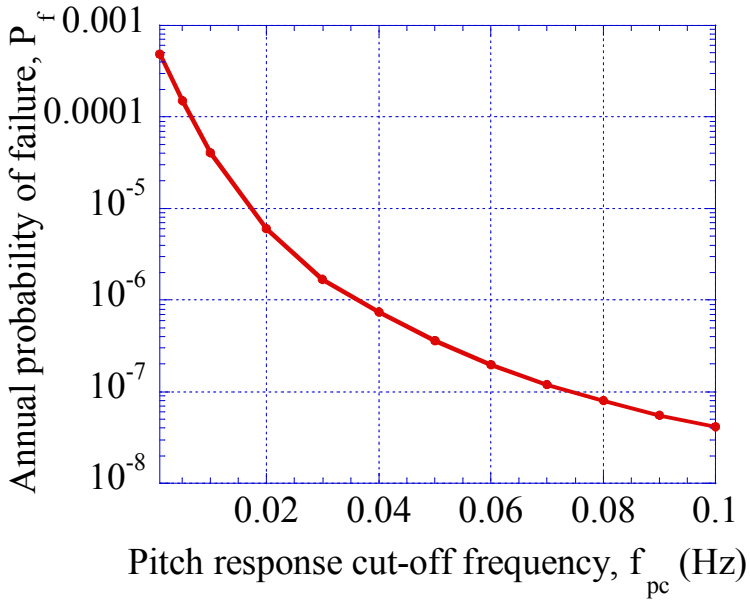

Figure 8. Annual probability of bending failure of the rotor blade vs. pitch response cut-off frequency.

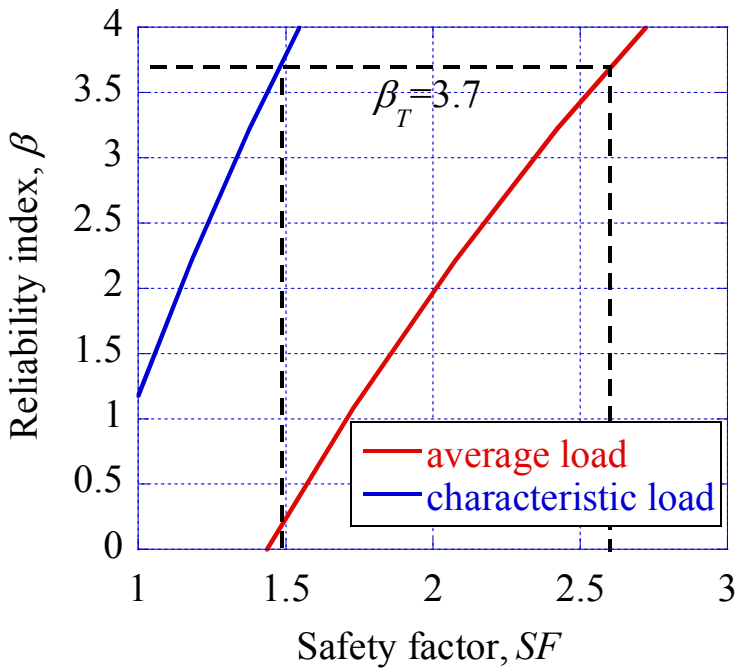

Figure 9. Reliability index vs. safety factor.